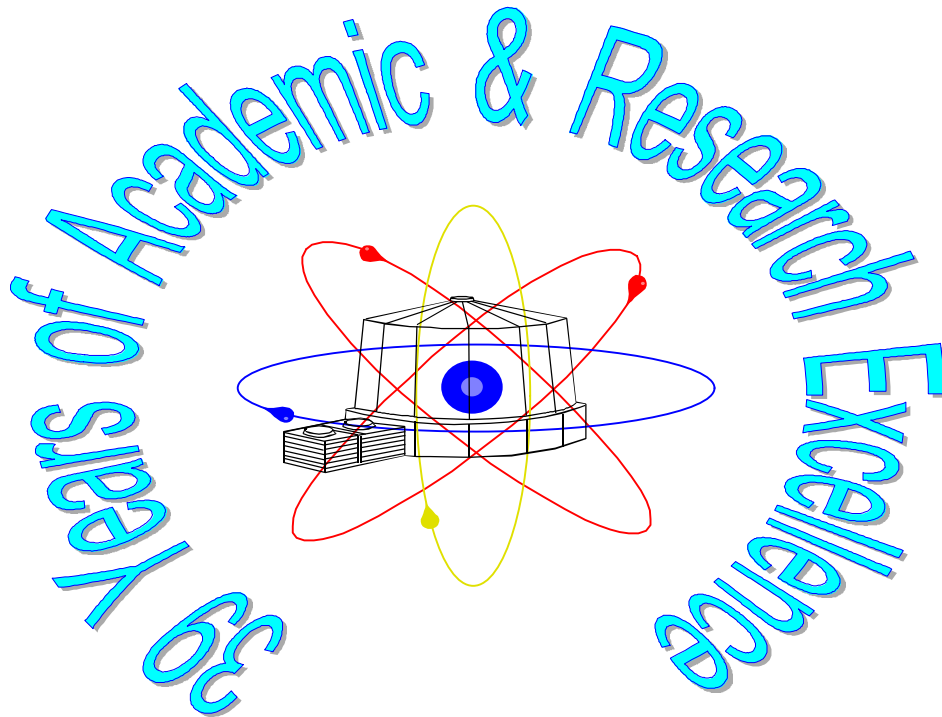


McMaster Nuclear Reactor
McMaster University
1280 Main Street West
Hamilton, Ontario L8S 4K1

(905) 525-9140 Ext 24065
Fax: (905) 528-4339

Technical Report 1999-01

Heat Transfer Limits for the McMaster Nuclear Reactor



Prepared by: _____ Date: _____
Wm. J. Garland, Reactor Analyst

Reviewed by: _____ Date: _____
M. Butler, Chief Reactor Supervisor

Approved by: _____ Date: _____
Frank Saunders, Reactor Manager

February 17, 1999

Heat Transfer Limits for the McMaster Nuclear Reactor

1 Introduction

Heat transfer considerations for MNR plate type fuel assemblies were introduced in [TR98-07]. Therein, it was argued that the onset of bulk boiling was the appropriate heat transfer limit for the low pressure, low velocity conditions at MNR. However, given that the onset of nucleate boiling (ONB) occurs before the onset of bulk boiling and that elevated sheath temperatures occur at ONB, further investigation is warranted to ensure that fuel damage does not occur at thermalhydraulic conditions below bulk boiling. Herein, ONB, flow instability and DNB (departure from nucleate boiling) are investigated.

For clarity and reader convenience, the discussion in [TR98-07] on heat transfer and critical heat flux are repeated in the next two sections.

2 Heat Transfer Overview

Convective heat transfer is strongly dependent on the hydraulics, notably on velocity and flow regime, as well as on the material properties. MNR operates exclusively in single phase liquid mode under normal operation. The coolant is normally highly subcooled, even near the fuel sheath surface. If coolant flow is impaired sufficiently or if power should rise sufficiently, the coolant - sheath interface temperature will rise to or above the saturation temperature of the coolant (117°C in this case). To get a feel for the system response at the onset of bulk boiling, consider the simple coolant energy balance:

$$Q = W (h_{\text{sat liq}} + x h_{\text{fg}} - h_{\text{inlet}})$$

where Q = assembly power, kW
 W = assembly mass flow, kg/s
 x = assembly exit quality, fraction
 $h_{\text{sat liq}}$ = saturation enthalpy, kJ/kg
 h_{fg} = latent heat of vapourization, kJ/kg
 h_{inlet} = inlet enthalpy, kJ/kg.

If

$$\begin{aligned} Q_{\text{sat}} &= W (h_{\text{sat liq}} - h_{\text{inlet}}) \\ &\approx 2.25 \text{ kg/s} (490.5 - 125.8) \text{ kJ/kg} \approx 820 \text{ kW} \text{ (2 MW nominal conditions)} \\ &\approx 3.0 \text{ kg/s} (490.5 - 125.8) \text{ kJ/kg} \approx 1100 \text{ kW} \text{ (5 MW nominal conditions)} \end{aligned}$$

is the assembly power required to bring the coolant up to saturation temperature, then

$$Q_{\text{two phase}} = W (x h_{\text{fg}})$$

is the relationship between the bulk quality and the power associated with boiling. At 2 MW, we have for a high power assembly: $Q \sim 125 \text{ kW}$, $W \sim 2.25 \text{ kg/s}$ and $h_{\text{fg}} \sim 2225 \text{ kJ/kg}$. Hence, a 1% increase in power beyond that needed to bring the coolant to saturation will generate a quality of $0.01 \times 125 \text{ kW} / (2.25 \text{ kg/s} \times$

2225kJ/kg) = 0.00025 weight fraction. This is a very small amount of quality but, from steam tables, the density of steam at 180 kPa is almost 1000 times the liquid volume. The void fraction equivalent of this quality is 0.20, ie 20% by volume of the coolant is vapour. Note also that, from the heat balance above, an overpower of about 6.5 times (depending on assembly mass flow) will generate bulk boiling. Hence we expect the critical heat flux (CPR) to be at least 6.5 based on bulk boiling being an early indicator of a heat transfer crisis.

Vapour generation in the coolant is not a crisis in itself but the onset of significant vapour quality yields large voids (since the system pressure and coolant velocities are low) and possible flow instabilities, vapour blanketing and sheath dryout. The transition from nominal cooling to a heat transfer crisis is sharp and is not easily modelled. Hence, for MNR, it is assumed herein, to be conservative, that the onset of significant boiling represents a safety limit. It follows that it is more meaningful to focus on the determination of the heat transfer coefficient rather than the critical heat flux so as to be able to predict the sheath surface temperature's approach to saturation as accurately as possible during event scenarios. Consequently, herein, we are concerned primarily with single phase liquid flow heat transfer.

For MNR 18 plate assemblies at 2 MW nominal conditions:

velocity, $v = 0.73$ m/s

equivalent hydraulic diameter, $De = 0.55$ cm

density, $\rho = 947$ kg/m³

dynamic viscosity, $\mu = 238 \times 10^{-6}$ kg/m-s [HAA84]

heat capacity, $C_p = 4.2 \times 10^3$ J/kg°C [HAA84]

heat conductivity, $k = 0.68$ W/m°C [HAA84]

Hence Reynolds number, $Re = \rho v De / \mu \approx 16,000$. According to Incropera [INC90, pg 457], the onset of turbulence occurs at Re of about 2,300 with fully turbulent flow by Re of 10,000. Hence we can safely assume that the nominal core flow is turbulent.

The Prandtl number, $Pr = \mu C_p / k = 1.47$.

For turbulent flow it is acceptable to use pipe correlations for channel flow [INC90, pg 461]. The Dittus Boelter correlation, Nu (Nusselt number = $h De / k$) = $0.023 Re^{0.8} Pr^{0.4} = 61.9$, where h is the heat transfer coefficient, is appropriate. For the values of De and k above, a Nu of 61.9 translates into an h of approximately 7600 W/°C. The recommended heat transfer correlation (default) in CATHENA is the modified Chen correlation which provides a smoother transition between heat transfer regimes. Typical h values generated by CATHENA are in the range of 6000 to 8000 W/°C.

For laminar flow, such as might occur under thermosyphoning conditions, pipe correlations are not applicable. However, $Nu \sim 6.49$ to 8.23 for a channel width to thickness ratio of 8 or greater [INC90, pg 461] (MNR plate assemblies have a width to thickness ratio of 23 for 18 plate fuel and 10 for the 10 plate fuel). Note that for laminar flow, Nu , and hence h , is independent of velocity; that is, the heat transfer is solely determined by heat conduction through the boundary layer. CATHENA uses the turbulent correlation (modified Chen in this case) in general but reverts to a limiting Nu of 3.66 at low flows, consistent with the above observations.

For thermosyphoning, the flow in a channel will be governed by the channel density (ie local power) and the

overall channel resistance (dominated by the exit and entrance losses of the assembly). The resistance through the plenum and flapper hole is negligible. Channel flow instabilities are possible at or near boiling since parallel channels exist and hydraulic resistances are low.

In summary, for forced flow in narrow channels, pipe correlations such as Dittus Boelter can be used. For laminar flow, the Nusselt number is constant, ie heat transfer is independent of velocity. Thus, for forced flow we know velocity (see [TR98-07], sections 5.6 and 5.9) and we have a reliable heat transfer correlation. For laminar flow the velocity is uncertain but we do not need to know it to get the nominal heat transfer coefficient. Since a fuel sheath surface temperature close to the coolant saturation temperature is a good indication of the approach to dryout, an exact knowledge of CHF is not necessary.

3 Critical Heat Flux

To support the above approach, CHF correlations for plate geometries were investigated. The only correlation supported by CATHENA that is suitable for plate geometries is that of Mirshak [MIR59]. Mishima [MIS87] provides an excellent review of CHF for low velocity and pressure situations, including channel flow. Mishima compares various CHF correlations and shows the Mirshak correlation to be comparable to others in its range of applicability (5 to 45 ft/s, 5-75 °C subcooling, 25-85 psia, De 0.21-0.46", vertical downflow, channel geometry - all suitable to MNR plate type assemblies at nominal power conditions except for velocity).

The Mirshak correlation (CATHENA Theoretical Manual, pg A-18) [CAT95] is:

$$q''_{CHF} = 1.51 \times 10^6 [1 + 0.1197 v_m] [1 + 9.14 \times 10^{-3} \Delta T] [1 + 1.896 \times 10^{-1} P]$$

where

$$v_m = \frac{G_{mix}}{\alpha_g \rho_g + [1 - \alpha_g] \rho_f} \quad \text{m/s}$$

P = total pressure, Bar
 $\Delta T = \max[0, T_f^{sat} - T_f] \quad \text{°C}$

For MNR 18 plate assemblies:

$$\begin{aligned} v_m &\approx 0.73 \text{ m/s} \\ P &\approx 1.8 \text{ Bar} \\ \Delta T &\approx 0 \text{ °C} \end{aligned}$$

giving a CHF of $\sim 2.17 \times 10^6 \text{ J/m}^2\text{s}$. The nominal peak heat flux is $\sim 0.11 \times 10^6 \text{ J/m}^2\text{s}$ giving a CPR of ~ 19.7 . This is agreement with CATHENA output (CPR ~ 21), given the differences in nodalization and correlations. Note that velocity, and hence v_m will vary from case to case but the correlation is not particularly sensitive to variations in v_m (a 10% variation in v_m gives $\sim 1\%$ variation in CHF). To assess the applicability of the Mirshak correlation at velocities lower than 5 ft/s (1.5 m/s), we turn to Mishima's comparison of the Mirshak correlation to other correlations. Mishima defines a dimensionless volumetric mass flow

$$G^* \equiv \frac{G}{\sqrt{\lambda \rho_g g \Delta \rho}}$$

and a dimensionless heat flux

$$q^* \equiv \frac{q}{h_{fg} \sqrt{\lambda \rho_g g \Delta \rho}}$$

where

$$\lambda = \sqrt{\frac{\sigma}{g \Delta \rho}} \text{ and } \sigma = \text{surface tension}$$

The MNR values are

$$\lambda = \sqrt{\frac{0.055 \text{ kg/s}^2}{9.81 \text{ m/s}^2 \times 946 \text{ kg/m}^3}} = 0.00243 \text{ m}$$

$$G^* \equiv \frac{947 \times 0.73}{\sqrt{0.00243 \times 0.948 \times 9.81 \times 947}} = 947 \times 0.73 / 4.63 = 149.3$$

$$q^*_{CHF} \equiv \frac{2.17 \times 10^6}{2225 \times 10^3 \sqrt{0.00243 \times 0.948 \times 9.81 \times 947}} = 0.210$$

These values correspond to the extreme lower limit of Mirshak's correlation as plotted by Mishima in his figure 8 (q^* vs G^*). Judging by the other correlations evaluated on the same plot, we would expect the Mirshak correlation to yield CHF values that are too high for velocities below 1.5 m/s. This is consistent with the premise that a heat transfer crisis occurs soon after the onset of significant void and that bulk outlet boiling starts at roughly 6.5 times nominal power, based on the simple heat balance presented at the beginning of this report. Mishima shows that dryout occurs at ~ 0 exit quality under these conditions, confirming the assertion made herein that at low pressure and flow, if significant boiling occurs, a heat transfer crisis is not far off. In effect, exact knowledge of CHF is not required for MNR and, hence, the high predictions of the Mirshak correlation at low velocities is inconsequential.

It is sufficient to have a heat transfer coefficient that is sufficiently accurate to determine the sheath surface temperature since it is the sheath temperature that determines the onset of boiling (it must at least be the saturation temperature of $\sim 117^\circ\text{C}$) and, in the extreme (temperatures $> \sim 450^\circ\text{C}$), fuel failure. Significant boiling can lead to flow instabilities for MNR type conditions [MIS87]. CATHENA simulations typically break down under these conditions because of the large volumetric expansion of the vapour phase and the low hydraulic resistances in the parallel paths of the core.

As mentioned at the beginning, given that the onset of nucleate boiling (ONB) occurs before the onset of bulk boiling and that elevated sheath temperatures occur at ONB, further investigation is warranted to ensure that fuel damage does not occur at thermalhydraulic conditions below bulk boiling. ONB, flow instability and DNB (departure from nucleate boiling) are investigated in turn.

4 Onset of Nucleate Boiling

The onset of nucleate boiling (ONB) under low pressure low flow conditions is a measure of the approach to a heat transfer crisis, although it is, itself, not a heat transfer crisis. The phenomena has been investigated for MNR conditions in detail by the IAEA [TECDOC-233] and confirmed by experiments. The IAEA recommends the Bergles and Rohsenow correlation for the sheath temperature at which ONB occurs:

$$T_{s-\text{onb}} = T_{\text{sat}} + \frac{5}{9} \left(\frac{9.23 q''}{P^{1.156}} \right)^{\left(\frac{P^{0.0234}}{2.16} \right)}$$

where $T_{s-\text{onb}}$ = sheath surface temperature, °C, at which ONB occurs
 T_{sat} = saturation temperature, ~117 °C for MNR conditions
 q'' = local heat flux, W/cm²
 P = local pressure, bar abs.

The actual local sheath surface temperature is given from the definition of the heat transfer coefficient:

$$q'' = h (T_{\text{fluid}} - T_s)$$

since the local heat flux q'' and the bulk fluid temperature is known and since the heat transfer coefficient, h , can be calculated from the Dittus Boelter correlation:

$$\text{Nu} \text{ (Nusselt number} = h \text{ De}/k) = 0.023 \text{ Re}^{0.8} \text{Pr}^{0.4}$$

or any other appropriate correlation (CATHENA recommends the modified Chen correlation since it has been shown to be applicable over a broader range of operating condition, including boiling).

The question is: “At what power will the actual sheath surface temperature somewhere in the core reach or exceed $T_{s-\text{onb}}$, the temperature at which ONB will occur?” To find this power, some iteration is required. The procedure then, is, starting from nominal conditions, calculate the fluid temperature and the sheath surface temperature along the channel, and compare the sheath surface temperature to that of $T_{s-\text{onb}}$. If $T_s < T_{s-\text{onb}}$ everywhere in the core, margin to ONB exists and the reactor power can be increased, thereby increasing q'' . The calculation is repeated until the margin drops to 0. The ratio of Power at ONB to nominal power is a measure of the margin to ONB.

The above correlations and procedure has been confirmed to be appropriate for MNR by Oak Ridge Research Reactor experiments and COBRA calculations [TECDOC-233].

This calculation was performed for MNR for nominal conditions at 2 MW and 5 MW. The margins were found to be 3.82 and 2.15 respectively. This is well above the 1.25 FP trip setting at MNR. See appendix 1 for details on the spreadsheet calculations. Figure 1 shows the temperature profiles at ONB.

A number of CATHENA simulations (runs onb2a and 3a) were performed for comparison purposes (see appendix 2 for archival information). For the 2 MW nominal power case, at 3.90 times overpower, CATHENA predicts a sheath temperature of 124 °C, in agreement with the spreadsheet calculation. For the 5 MW nominal power case, at 2.15 times overpower, CATHENA predicts a sheath temperature of 126 °C, in agreement with the spreadsheet calculation.

5 Flow Instability

Flow instability was also investigated by the IAEA [TECDOC-233]. It was found that density wave oscillations are not a concern for research reactors operating at near atmospheric conditions. But flow excursions of the Ledinegg type can occur at a sufficiently high heat flux. It was determined that the flow excursions were not sensitive to the shape of the axial flux profile. Experiments by Whittle and Forgan on assemblies similar to MNR led to their estimate of flow instability occurring at an average heat flux of

$$q_{c-avg} = R \rho C_p \left(\frac{W}{W_H} \right) \left(\frac{t_w}{L_H} \right) v (T_{sat} - T_{in})$$

$$\text{where } R = \frac{1}{1 + \eta \frac{D_H}{L_H}}$$

where ρ is the fluid density, kg/m³,
 C_p is the heat capacity, J/kg °C,
 v = velocity, m/s,
 T_{sat} = the fluid saturation temperature, ~117 °C,
 T_{in} = channel inlet temperature, °C,
 W = fuel plate width, m,
 W_H = heated width, m,
 t_w = channel thickness (plate separation), m,
 L_H = heated length,
 and $\eta = 25$ (experimental fit parameter).

For MNR at 2 MW and 5MW, this correlation predicts flow instability margins of 9.53 and 5.55 times overpower, respectively.

A second correlation offered by [TECDOC-233] is that of Winkler:

$$q_{c-avg} = -29.35 + (1.2815 - 1.104 T_{in}) v^{0.8}$$

which is based on the data of Forgan and Whittle plus burnout data by Fried, Hofman and Peterson. For MNR at 2 MW and 5MW, this correlation predicts flow instability margins of 4.20 and 2.69 times overpower, respectively. This is roughly a factor of 2 lower than what the Whittle and Forgan correlation predicts but still significantly beyond ONB.

CATHENA simulations (runs onb5a and 6a) give flow instability for the 2 MW and 5 MW cases as just over 6.0 and 3.2 times overpower, ie falling in between the predictions of the two correlations. In the CATHENA simulations, flow instabilities occur the moment the fluid reaches the saturation temperature and bulk boiling occurs. Given the channel flow and fluid properties, the overpower margin to bulk boiling can be directly calculated. Hand calculations give a ratio of 6.5 and 3.5 times nominal power for the 2 MW case and the 5 MW case, consistent with the more refined CATHENA calculation. There are slight differences in the assembly flows in CATHENA compared to that used in the hand calculations (about 5% lower in the CATHENA runs); the exact assembly velocity varies, depending on the heat transport valve settings and the core makeup.

6 Departure from Nucleate Boiling

In addition to ONB and flow instability, the IAEA investigated departure from nucleate boiling (DNB) [TECDOC-233]. The correlations of Mirshak and Labuntsov were found to be the best suited to low pressure plate type research reactors like MNR.

The Mirshak correlation has been given previously in section 2. The Labuntsov correlation states:

$$q_{\text{dnb}} = 145.4 \theta \left(\frac{12.5 v^2}{\theta} \right)^{1/4} \left(1 + 15.1 C_p \frac{\Delta T_{\text{sub}}}{h_{\text{fg}} P^{1/2}} \right)$$

$$\text{where } \theta = 0.99531 P^{1/3} \left(1 - \frac{P}{P_c} \right)^{4/3}$$

and where P_c is the critical pressure, ΔT_{sub} is the exit subcooling and h_{fg} is the heat of vapourization. Although these correlations were strictly applicable to velocities above 2 m/s, they extrapolated well to the Roshenow and Griffith pool boiling CHF correlation if the exit subcooling were set to 0. With this restriction, the Mirshak correlation gave DNB margins of 18.4 and 7.63 times nominal power for MNR at 2 MW and 5 MW respectively. The Labuntsov correlation yielded 17.35 and 7.75 quite close to that of the Mirshak correlation. As expected, flow instability occurs well before DNB at the low pressure, low velocity conditions of MNR. A comparison to CATHENA (or, indeed, any such modelling code) could not be performed because flow instability is reached before DNB.

7 Conclusions

To conclude this investigation of heat transfer limitations of MNR, hand calculations, available correlations and CATHENA simulations consistently indicate that:

1. ONB is not a phenomena of concern since the sheath temperatures at ONB of about 125 °C are well below temperatures at which sheath blistering or swelling occur (400 to 450 °C).
2. Flow instability occurs at the onset of bulk boiling and can be reliably estimated given a good channel velocity estimate.
3. DNB follows somewhat after flow instability(perhaps at twice the power) , hence bulk boiling can be conservatively used as a limiting condition for safety analysis.

References

CAT95 -, "CATHENA MOD-3.5 / Rev 0, Theoretical Manual", Atomic Energy of Canada Limited, ed. B.N. Hanna, RC-982-3, 1995.

HAA84 L. Haar, J. Gallagher and G Kell, 1984 NBS/NRC Steam Tables, McGraw-Hill International, Toronto.

INC90 Frank P. Incropera and Davis P. DeWitt, Introduction to Heat Transfer, John Wiley & Sons, Second Edition, ISBN 0-471-61247-2.

MIR59 S. Mirshak, W.S. Durant, and R.H. Towell, "Heat Flux at Burnout," AEC R&D Report DP-355, E.I. du Pont de Nemours & Co., Aiken, South Carolina, 1959 February.

MIS87 K. Mishima and H. Nishihara, "Effect of Channel Geometry on Critical Heat Flux for Low Pressure Water," Int. J. of Heat & Mass Transfer, Vol. 30, No. 6, 1169-1182 (1987 June)

TECDOC-233 -, "Research Reactor Core Conversion from the Use of Highly Enriched Uranium to the Use of Low Enriched Uranium Fuels Guidebook", IAEA TECDOC-233, 1980.

TR 1997-04 Wm. J. Garland, "Thermalhydraulic Modelling of MNR", McMaster University Nuclear Reactor, Technical Report MNR-TR 97-04, approx. 60 pages, June 15, 1997.

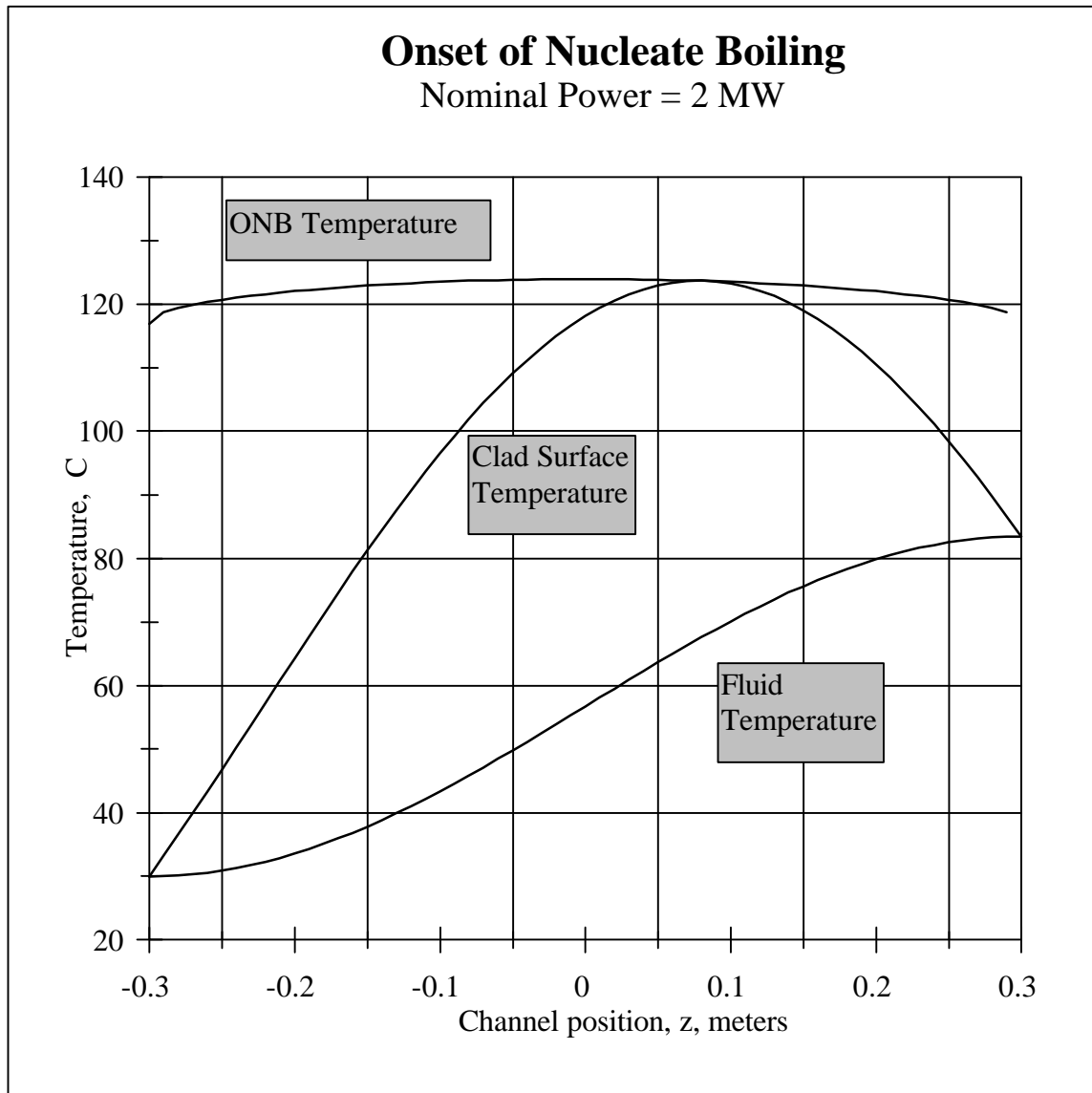


Figure 1 Axial temperature profiles at the onset of nucleate boiling for the 2 MW nominal power case. ONB occurs at 7.64 MW. The curves for the 5 MW case are virtually identical. ONB for 5 MW nominal conditions occurs at 10.77 MW.

Appendix 1 Spreadsheet Calculations for ONB, Flow Instability and DNB

1.1 Nominal Power of 2 MW

Onset of Nucleate Boiling (ONB) for MNR				file: d:\mnr\aecb\thanal\htlimit\htlimit1at2Mrev2.wb3 1999-02:16					
based on IAEA TECDOC 233				Axial calculation					
Input data				z	q(z)	Tfluid(z)	Ts(z)	Tonb	Tonb-Ts
tw	0.00289	metres	Channel thickness	-0.3	2.7E-11	30	30	117	87
Wh	0.06632	metres	Channel width	-0.29	23499.5	30.0367	33.2508	118.761	85.5105
De	0.0055	metres	Equivalent diameter of channel	-0.28	46934.7	30.1465	36.5661	119.436	82.8699
Nc	17		Number of coolant channels	-0.27	70241.2	30.3293	39.9366	119.943	80.0061
Ac	0.0032583	m^2	Assembly flow area	-0.26	93355.1	30.5845	43.3533	120.362	77.0092
Hco	0.6	metres	Heated length	-0.25	116213	30.9114	46.8066	120.726	73.9195
Nf	16		Number fuel plates	-0.24	138753	31.3091	50.2872	121.049	70.7617
Cp	4200	J/kgC	Water heat capacity	-0.23	160912	31.7765	53.7854	121.34	67.5547
mu	0.000238	kg/m-s	Dynamic Viscosity	-0.22	182630	32.3123	57.2918	121.605	64.3136
rho	947	kg/m^3	Water density	-0.21	203848	32.9152	60.7967	121.849	61.0522
k	0.68	W/m-C	Water conductivity	-0.2	224507	33.5833	64.2905	122.073	57.7829
v	0.69	m/s	Velocity	-0.19	244550	34.315	67.7637	122.281	54.5173
P	1.7029703	bar	Pressure	-0.18	263923	35.1081	71.2066	122.473	51.2665
Tin	30	C	Inlet temperature	-0.17	282573	35.9605	74.6099	122.651	48.0412
Nass	35		Number of fuel assemblies	-0.16	300449	36.8699	77.9642	122.816	44.8517
Tsat	117	C	Saturation temperature	-0.15	317500	37.8338	81.2604	122.968	41.708
Qnominal	2.000E+06	watts	Nominal core power	-0.14	333682	38.8495	84.4894	123.109	38.6198
Qhotass	125000	watts	Hot assembly power	-0.13	348949	39.9143	87.6423	123.239	35.5963
				-0.12	363260	41.0252	90.7105	123.357	32.6467
				-0.11	376574	42.1792	93.6857	123.465	29.7797
				-0.1	388857	43.3731	96.5596	123.563	27.0038
				-0.09	400074	44.6037	99.3244	123.652	24.3271
				-0.08	410194	45.8676	101.972	123.73	21.7574
				-0.07	419190	47.1613	104.497	123.799	19.3021
				-0.06	427037	48.4812	106.89	123.858	16.9682
				-0.05	433714	49.8238	109.146	123.908	14.7624
				-0.04	439201	51.1854	111.258	123.949	12.6911
				-0.03	443485	52.5623	113.221	123.981	10.76
				-0.02	446554	53.9505	115.029	124.003	8.97466
				-0.01	448398	55.3465	116.677	124.017	7.33998
				1.4E-16	449013	56.7463	118.161	124.021	5.86053
				0.01	448398	58.1461	119.476	124.017	4.54039
				0.02	446554	59.542	120.62	124.003	3.38316
				0.03	443485	60.9303	121.589	123.981	2.39195
				0.04	439201	62.3072	122.38	123.949	1.56937
				0.05	433714	63.6687	122.991	123.908	0.91754
				0.06	427037	65.0114	123.42	123.858	0.43807
				0.07	419190	66.3313	123.667	123.799	0.13204
				0.08	410194	67.625	123.73	123.73	4.1E-07
				0.09	400074	68.8889	123.61	123.652	0.042
				0.1	388857	70.1194	123.306	123.563	0.25754
				0.11	376574	71.3134	122.82	123.465	0.64558
				0.12	363260	72.4674	122.153	123.357	1.20455
				0.13	348949	73.5783	121.306	123.239	1.93233
				0.14	333682	74.6431	120.283	123.109	2.82624
				0.15	317500	75.6588	119.085	122.968	3.88307
				0.16	300449	76.6227	117.717	122.816	5.09901
				0.17	282573	77.5321	116.181	122.651	6.46968
				0.18	263923	78.3845	114.483	122.473	7.99009
				0.19	244550	79.1776	112.626	122.281	9.65463
				0.2	224507	79.9093	110.616	122.073	11.457
				0.21	203848	80.5774	108.459	121.849	13.39
				0.22	182630	81.1802	106.16	121.605	15.4457
				0.23	160912	81.7161	103.725	121.34	17.615
				0.24	138753	82.1835	101.162	121.049	19.8873
				0.25	116213	82.5812	98.4765	120.726	22.2496
				0.26	93355.1	82.9081	95.6769	120.362	24.6856
				0.27	70241.2	83.1633	92.7706	119.943	27.1721
				0.28	46934.7	83.3461	89.7656	119.436	29.6703
				0.29	23499.5	83.4559	86.6701	118.761	32.0912
				0.3	-6.7E-10	83.4926	83.4926	ERR	ERR
ONB calculation									
Tsonb	124.021269	C	Sheath T for ONB (Bergles & Rohsenow)						
Ts	144.907032	C	Conservative estimate of sheath temp (eqn 14)						
Ts(z)max	123.729879	C	Calculated sheath temp (eqns 12 & 13)						
Tsonb-Ts(z)min	4.1E-07								
fp	3.82668952		Margin to ONB						
Procedure:									
			Vary fp until Ts(z)max = Ts onb						
			Can do manually or use solver						
Powers, fluxes and Temperatures at ONB									
Qcore	7.653E+06	watts	Core power						
Qassaver	218667.973	Watts	Average assembly power						
Qassmax	478336.19	Watts	Peak assembly power						
qa	171727.336	W/m^2	Average heat flux						
q0	449013.47	W/m^2	Peak heat flux						
Toutaver	54.4537539	C	Outlet T based on overall heat balance for average assembly						
Toutpeak	83.4925866	C	Outlet T based on overall heat balance for peak assembly						

Onset of Flow Instability for MNR				
based on IAEA TECDOC 233				
Input data				
neta	25			
Derived data				
Forgan correlation				
R	0.81356		eqn 19	of [TECDOC-233]
qcaverf	935628	W/m ²	eqn 20	of [TECDOC-233]
qcpeakf	1118344			
	9.53102		Margin to flow instability	
Winkler correlation				
qcaver	412720	W/m ²	eqn 21	of [TECDOC-233]
qcpeak	493318	W/m ²		
	4.20428		Margin to flow instability	

Onset of Departure from Nucleate Boiling (DNB) for MNR				
based on IAEA TECDOC 233				
Input data				
Pc	207.921	Bar	Critical pressure	
hfg	2200	kJ/kg	Latent heat of vapourization	
Derived data				
dTsub	0	C	Exit subcooling when q=qc	
theta	1.17561			
qclab	2035920	W/cm ²	Heat flux at DNB (Labuntsov correlation)	
	17.351		Margin to DNB	
qcmir	2163789	W/cm ²	Heat flux at DNB (Mirshak correlation)	
	18.4408		Margin to DNB	

1.2 Nominal Power of 5 MW

Onset of Nucleate Boiling (ONB) for MNR				file: d:\mnr\aecb\thana\htlimit\htlimit1at5Mrev2.wb3 1999:02:16						
based on IAEA TECDOC 233				Axial calculation						
Input data				z	q(z)	Tfluid(z)	Ts(z)	Tonb	Tonb-Ts	
tw	0.00289	metres	Channel thickness	-0.3	3.9E-11	30	30	117	87	
Wh	0.06632	metres	Channel width	-0.29	33070.4	30.0355	33.3869	119.067	85.6803	
De	0.0055	metres	Equivalent diameter of channel	-0.28	66050.2	30.1417	36.8354	119.859	83.0236	
Nc	17		Number of coolant channels	-0.27	98848.9	30.3186	40.3361	120.454	80.1177	
Ac	0.0032583	m^2	Assembly flow area	-0.26	131377	30.5654	43.8794	120.947	77.0671	
Hco	0.6	metres	Heated length	-0.25	163544	30.8816	47.4556	121.373	73.9177	
Nf	16		Number fuel plates	-0.24	195264	31.2664	51.0548	121.752	70.6973	
Cp	4200	J/kgC	Water heat capacity	-0.23	226448	31.7186	54.6673	122.094	67.4267	
mu	0.000238	kg/m-s	Dynamic Viscosity	-0.22	257012	32.2369	58.283	122.405	64.1224	
rho	947	kg/m^3	Water density	-0.21	286871	32.8201	61.8922	122.691	60.799	
k	0.68	W/m-C	Water conductivity	-0.2	315944	33.4665	65.4849	122.955	57.4698	
v	1.004	m/s	Velocity	-0.19	344150	34.1743	69.0512	123.198	54.147	
P	1.703	bar	Pressure	-0.18	371414	34.9415	72.5814	123.424	50.8423	
Tin	30	C	Inlet temperature	-0.17	397659	35.7662	76.0658	123.633	47.5669	
Nass	35		Number of fuel assemblies	-0.16	422815	36.6459	79.4949	123.826	44.3313	
Tsat	117	C	Saturation temperature	-0.15	446812	37.5784	82.8592	124.005	41.1459	
Qnominal	5.000E+06	watts	Nominal core power	-0.14	469584	38.561	86.1496	124.17	38.0207	
Qhotass	312500	watts	Hot assembly power	-0.13	491068	39.591	89.357	124.322	34.9653	
				-0.12	511207	40.6657	92.4726	124.461	31.9889	
				-0.11	529945	41.7821	95.4879	124.588	29.1006	
				-0.1	547230	42.9371	98.3946	124.703	26.3089	
				-0.09	563015	44.1276	101.185	124.807	23.6221	
				-0.08	577258	45.3502	103.851	124.899	21.0481	
FLOWass	3.09718266	kg/s	Assembly flow	-0.07	589917	46.6017	106.385	124.98	18.5944	
MassFlux	950.55125	kg/m^2-s	Assembly mass flux	-0.06	600960	47.8786	108.781	125.049	16.268	
Re	21966.5205		Reynolds number	-0.05	610356	49.1775	111.032	125.108	14.0757	
Pr	1.47		Prandtl number	-0.04	618079	50.4947	113.132	125.156	12.0238	
Nu	79.8111899		Nusselt number	-0.03	624107	51.8266	115.075	125.193	10.1181	
h	9867.5653	W/C	Heat transfer coefficient	-0.02	628426	53.1696	116.856	125.22	8.36404	
				-0.01	631021	54.5201	118.469	125.236	6.76646	
				1.4E-16	631887	55.8742	119.911	125.241	5.32984	
Qaverass	142857.143	watts	Average assembly power	0.01	631021	57.2284	121.177	125.236	4.05816	
qanom	112190.534	W/m^2	Nominal average heat flux	0.02	628426	58.5788	122.665	125.22	2.95486	
qOnom	293343.285	W/m^2	Nominal peak heat flux	0.03	624107	59.9218	123.17	125.193	2.02291	
Toutaver	40.9821115	C	Outlet T based on overall heat balance for average assembly	0.04	618079	61.2538	123.891	125.156	1.26474	
Toutpeak	54.023369	C	Outlet T based on overall heat balance for peak assembly	0.05	610356	62.571	124.426	125.108	0.68226	
Tr	2.1875		Radial peak to average	0.06	600960	63.8698	124.772	125.049	0.27686	
fa	1.19528612		Axial peak to average, chopped cosine	0.07	589917	65.1467	124.93	124.98	0.04938	
f	2.61468838		Core peak to average	0.08	577258	66.3982	124.899	124.899	0.00012	
				0.09	563015	67.6209	124.678	124.807	0.12882	
				0.1	547230	68.8113	124.269	124.703	0.43469	
				0.11	529945	69.9663	123.672	124.588	0.91637	
				0.12	511207	71.0827	122.89	124.461	1.57194	
				0.13	491068	72.1574	121.923	124.322	2.3989	
				0.14	469584	73.1874	120.776	124.17	3.39421	
				0.15	446812	74.1701	119.451	124.005	4.55422	
				0.16	422815	75.1025	117.951	123.826	5.87469	
				0.17	397659	75.9823	116.282	123.633	7.35077	
				0.18	371414	76.8069	114.447	123.424	8.97698	
				0.19	344150	77.5742	112.451	123.198	10.7471	
				0.2	315944	78.2819	110.3	122.955	12.6543	
				0.21	286871	78.9283	108	122.691	14.6908	
				0.22	257012	79.5115	105.558	122.405	16.8478	
				0.23	226448	80.0299	102.979	122.094	19.1154	
				0.24	195264	80.4821	100.271	121.752	21.4817	
				0.25	163544	80.8668	97.4407	121.373	23.9325	
				0.26	131377	81.183	94.497	120.947	26.4495	
				0.27	98848.9	81.4299	91.4474	120.454	29.0064	
				0.28	66050.2	81.6067	88.3004	119.859	31.5587	
				0.29	33070.4	81.713	85.0644	119.067	34.0028	
				0.3	-9.4E-10	81.7484	81.7484	ERR	ERR	
ONB calculation										
Tsonb	125.240835	C	Sheath T for ONB (Bergles & Rohsenow)							
Ts	145.78521	C	Conservative estimate of sheath temp (eqn 14)							
Ts(z)/max	124.930187	C	Calculated sheath temp (eqns 12 & 13)							
Tsonb-Ts(z)/min	0.00012									
fp	2.15408734		Margin to ONB							
Procedure:										
			Vary fp until Ts(z)/max = Tsonb							
			Can do manually or use solver							
Powers, fluxes and Temperatures at ONB										
Qcore	1.077E+07	watts	Core power							
Qassaver	307726.763	Watts	Average assembly power							
Qassmax	673152.295	Watts	Peak assembly power							
qa	241668.208	W/m^2	Average heat flux							
q0	631887.057	W/m^2	Peak heat flux							
Toutaver	53.6564275	C	Outlet T based on overall heat balance for average assembly							
Toutpeak	81.7484351	C	Outlet T based on overall heat balance for peak assembly							

Onset of Flow Instability for MNR

based on IAEA TECDOC 233

Input data			
neta	25		
Derived data			
Forgan correlation			
R	0.81356	eqn 19	of [TECDOC-233]
qcaverf	1361068	W/m ²	eqn 20 of [TECDOC-233]
qcpeakf	1626866		
	5.54595	Margin to flow instability	
Winkler correlation			
qcaver	659650	W/m ²	eqn 21 of [TECDOC-233]
qcpeak	788470	W/m ²	
	2.68788	Margin to flow instability	

Onset of Departure from Nucleate Boiling (DNB) for MNR

based on IAEA TECDOC 233

Input data			
Pc	207.921	Bar	Critical pressure
hfg	2200	kJ/kg	Latent heat of vapourization
Derived data			
dTsub	0	C	Exit subcooling when q=qc
theta	1.17561		
qclab	2275879	W/cm ²	Heat flux at DNB (Labuntsov correlation)
	7.75842	Margin to DNB	
qcmir	2238910	W/cm ²	Heat flux at DNB (Mirshak correlation)
	7.63239	Margin to DNB	

Appendix 2 CATHENA Input and Output Files

Table of Contents:

Steady state overpower, 390% of 2 MW nominal power conditions:

onb2a.inp	Input file, defined power history for an HEU core.
onb2a-pk.out	Output file (selected core power parameters vs. time)
onb2a-mnrhot.out	Output file (selected 18 plate HEU assembly parameters vs. time)
onb2a-leuhot.out	Output file (selected 18 plate LEU assembly parameters vs. time)
onb2a-ptrhot.out	Output file (selected 10 plate assembly power parameters vs. time)
onb2a.lis	Full output listing
Archive directory (AECL-SP): herzberg:u94/garlandw/cathena/ovrpwr/rev1/ss.	

Steady state overpower, 600% of 2 MW nominal power conditions:

onb3a.inp	Input file, defined power history for an HEU core.
onb3a-pk.out	Output file (selected core power parameters vs. time)
onb3a-mnrhot.out	Output file (selected 18 plate HEU assembly parameters vs. time)
onb3a-leuhot.out	Output file (selected 18 plate LEU assembly parameters vs. time)
onb3a-ptrhot.out	Output file (selected 10 plate assembly power parameters vs. time)
onb3a.lis	Full output listing
Archive directory (AECL-SP): herzberg:u94/garlandw/cathena/ovrpwr/rev1/ss.	

Steady state overpower, 215% of 5 MW nominal power conditions:

onb5a.inp	Input file, defined power history for an HEU core.
onb5a-pk.out	Output file (selected core power parameters vs. time)
onb5a-mnrhot.out	Output file (selected 18 plate HEU assembly parameters vs. time)
onb5a-leuhot.out	Output file (selected 18 plate LEU assembly parameters vs. time)
onb5a-ptrhot.out	Output file (selected 10 plate assembly power parameters vs. time)
onb5a.lis	Full output listing
Archive directory (AECL-SP): herzberg:u94/garlandw/cathena/ovrpwr/rev1/ss.	

Steady state overpower, 320% of 5 MW nominal power conditions:

onb6a.inp	Input file, defined power history for an HEU core.
onb6a-pk.out	Output file (selected core power parameters vs. time)
onb6a-mnrhot.out	Output file (selected 18 plate HEU assembly parameters vs. time)
onb6a-leuhot.out	Output file (selected 18 plate LEU assembly parameters vs. time)
onb6a-ptrhot.out	Output file (selected 10 plate assembly power parameters vs. time)
onb6a.lis	Full output listing
Archive directory (AECL-SP): herzberg:u94/garlandw/cathena/ovrpwr/rev1/ss.	